

THE COMPUTER GENERATION OF ELECTRON MICROSCOPE PICTURES OF DISLOCATIONS

By A. K. HEAD*

[Manuscript received May 26, 1967]

Summary

For objects like dislocations, sufficient information to define a picture can be obtained in 1 min of numerical integration of the Howie-Whelan differential equations describing image formation in the electron microscope. To match this computational speed, the computer line printer is used to print pictures using the half-tone principle. Examples are given, including comparisons with experimental pictures, and it is concluded that when the important information is in the topology of the picture, rather than in precise intensities, a pictorial presentation of the theoretical calculations is valuable.

I. INTRODUCTION

Since the introduction of the two-beam column approximation of electron diffraction by Howie and Whelan (1961) there have been many calculations of the theoretical electron microscope images of various defects in crystals. The results of such calculations for dislocations have usually been presented as profiles of the variation of intensity along a line crossing the dislocation image. This is very appropriate if the experimental picture is microphotometered to produce the corresponding experimental profiles. However, this is not often done and more usually the theoretical profiles are mentally compared with a visual assessment of the experimental picture. Since it does not appear necessary to specify the exposure and contrast of such pictures to make this comparison and, moreover, since it is acceptable to adjust these photographic variables within reasonable limits to produce a good picture, it would appear that a large part of the useful information must lie in the topology of the picture. This being so it follows that it should be more valuable to present theoretical images as pictures rather than as profiles.

A method for the rapid computation of the large amount of information needed for a theoretical picture is described in Section II. To match this speed of computation, which averages 55 sec per picture, Section III describes the use of the computer line printer to produce a picture using the half-tone principle, in which the lights and shades are represented by small and large dots respectively.

II. COMPUTATIONS

We consider the case of a single straight dislocation sloping through a foil of thickness t and, for simplicity, assume that the foil normal and the electron beam

* Division of Tribophysics, CSIRO, University of Melbourne.

direction coincide.* The information necessary for a picture is that contained in a large number of profiles across the dislocation image when due account is taken of the geometry of projection of the three-dimensional object into a two-dimensional image. The fact that makes computer pictures of dislocations a practical proposition is that 65 profiles, which is more than sufficient for one picture, can be computed in essentially the same time as 4 profiles. This is because of the simple form of the elastic displacements around a straight dislocation and the linearity of the Howie-Whelan differential equations.

For either isotropic or anisotropic elasticity, the displacement field is such that along any line parallel to the dislocation the displacements are constant. This means that, instead of thinking of the different profiles as being due to the different displacements met by the beam in the corresponding cross sections of the foil, we can think of a generalized cross section with a fixed dislocation position and displacement field on which the variable positions of the foil surfaces delineate the different parts of this fixed field that the beam meets in the various profiles.

The equations of Howie and Whelan that describe this interaction of beam and displacement field are a pair of first-order linear differential equations for T and S , the amplitudes of the transmitted and scattered beams. There can be only two independent solutions of the equations, and if these are known then all other solutions must be linear combinations of them. The equations are integrated numerically from a distance t above the dislocation to a distance t below, the two solutions being recorded at steps of $t/64$. To guarantee two independent solutions, A and B , one run is started with $T_0^A = 1$ and $S_0^A = 0$ and the other with $T_0^B = 0$ and $S_0^B = 1$. Then T_{64}^A and S_{64}^A directly give a point on the bright and dark field profiles across the dislocation where it meets the bottom surface of the foil. The profile for the dislocation meeting the top surface is generated by choosing constants a and b such that

$$aT_{64}^A + bT_{64}^B = 1, \quad aS_{64}^A + bS_{64}^B = 0,$$

(corresponding to the physical beam starting at step 64 with $T = 1$ and $S = 0$) and then

$$T = aT_{128}^A + bT_{128}^B, \quad S = aS_{128}^A + bS_{128}^B$$

are the required amplitudes. Similarly 63 other profiles equally spaced between these two extremes are given, for $i = 1$ to 63, by

$$T = aT_{i+64}^A + bT_{i+64}^B, \quad S = aS_{i+64}^A + bS_{i+64}^B,$$

where

$$aT_i^A + bT_i^B = 1, \quad aS_i^A + bS_i^B = 0.$$

The number of profiles generated (65) is optimum in the following sense. The integration is performed by the well-known Runge-Kutta fourth order process using the modification by Merson (Lance 1960), which gives automatic choice of internal integration step size to meet a specified error criterion. If the allowable error is 0.0001 in the amplitudes per step then the natural internal step size for foils of

* The convention used in the present paper is that, for an untilted foil, the beam direction, the upward-drawn foil normal, and the upward-drawn plate normal are all identical, i.e. the beam direction is given on the "north wind convention" as the direction from which the electrons come.

thickness 3 to $5 \xi_g$ is in the range $t/35$ to $t/60$ over most of the integration (it of course becomes smaller very close to the dislocation). So the specified step of $t/64$ is usually done in one internal integration step. If steps of $t/32$ were used to generate 33 profiles then each external step would be broken down into two internal steps and very little time would be saved. On the other hand, if 129 profiles were calculated by using steps of $t/128$ then the computation time would be almost doubled by making the integration steps smaller than necessary. Typically, 65 profiles take 55 sec, 33 profiles 52 sec, and 129 profiles 105 sec for a Fortran programme on a CDC 3600 computer, which has times of 4.25 and $6.40 \mu\text{sec}$ for the addition and multiplication of floating point numbers.

From this same integration many other profiles or pictures can be generated for the dislocation in different thickness foils. If the values of the two solutions at points j steps apart are considered, instead of 64 steps apart, then $129-j$ profiles can be generated for a foil of thickness $jt/64$. If j is greater than 64 then all the profiles cross the dislocation line but are concentrated near the middle of the image. If j is less than 64 then $j+1$ profiles are uniformly distributed along the whole dislocation image, the other $128-2j$ profiles not crossing the dislocation line. Since, as is discussed in the next section, usable pictures can be generated with as few as 33 profiles, this means that, in essentially the same computer time as is necessary for 1 picture, 33 complete pictures can be generated for 33 foil thicknesses between $t/2$ and t .

Although the pictures that are considered in this paper are of single dislocations in an untilted foil, the same principles are applicable to a number of parallel dislocations, with or without faults connecting them, and also to tilted foils. However, the geometry of projection into a two-dimensional picture does become more complicated.

III. LINE PRINTER PICTURES

A typical line printer picture of a dislocation (for specifications, see Fig. 2(f)) is shown in Figure 1 together with the grey scale used. In order to get the blackest symbols it was found necessary to use overprinting. All combinations of printing and overprinting of the available symbols were examined and 11 different shades of grey could be distinguished, one of which was blank paper. The composition of the 10 printed shades chosen is shown in the grey scale. There are six lines of each symbol, the first and second columns being the individual characters and the third being the result when the first column is overprinted by the second. Most of the characters used are, of necessity, punctuation marks and other special symbols, since it is a characteristic of a good type face that letters and numerals do not have large differences in apparent blackness.

The standard picture size used is 60 lines of 129 symbols, which in the original is 10 by 13 in. The dislocation runs from left to right, intersecting the bottom surface of the foil at the left-hand margin of the picture and the top surface at the right margin. The line of the dislocation centre is located midway between the letters D on the right-hand margin. Due account is taken of the different spacings of characters along a line and between lines so that angles are true and linear scales are equal in all directions. The actual scale of the picture will depend on the foil thickness and the angle at which the dislocation slopes through the foil.

The standard picture contains 129 profiles of 60 points each. Of these, 65 equally spaced profiles are computed and 64 are interpolated. There is no difference between such a picture and one in which all 129 profiles are computed because the variation of intensity along lines parallel to the dislocation is always smooth. Even pictures with 33 calculated and 96 interpolated profiles are visually the same, although small differences can be found on close inspection, but since it takes almost no longer to calculate 65 profiles than 33 the former number is used. On the other hand, no interpolation is used along a profile as the intensity may have sharp changes in this direction.

The correspondence between value of intensity and shade of grey was determined by photometric measurements of the reflectivity R of large areas of the 11 shades. The corresponding intensity values I are then given by

$$\log I = \gamma^{-1} \log(R/E),$$

where the chosen values of the constants E and γ correspond to the photographic variables of exposure and contrast. The 10 boundary values indicated on the grey scale in Figure 1 were used for all of the present pictures. These values are not intensities as such but are the ratios of intensity to background. This means that all the pictures have the same contrast but each exposure is adjusted so that the background is always the first shade of grey. This appears a suitable choice for bright field pictures of dislocations, for which most of the information is in the regions darker than background and one shade, full white, is sufficient to represent those small areas that are significantly whiter than background. The contrast was chosen so that the values at which the background symbol changes (0.93 and 1.15) are approximately the experimental visibility limits for deviations from background. Different choices of exposure and contrast would be probably necessary for dark field pictures or if faults were present.

The main defect of the line printer is possible unevenness of the printing from column to column. With the orientation of the picture used here, these defects run perpendicular to the dislocation and have not been found to detract from the visual assessment of the originals. They would be more serious if they were to run parallel to the dislocation.

IV. DISCUSSION

We now consider the examples of computer-generated electron microscope images of dislocations shown in Figures 2-4. As many of the parameters are the same for these pictures, it is convenient to specify first those which are common. The anomalous absorption constant ξ_g/ξ'_g is taken as 0.1, being a value typical of metals. The pictures are independent of the value of the normal absorption ξ_g/ξ'_0 , as they depict intensities relative to background. The dislocation line is always along $[111]$. The material is β -brass in Figures 2 and 3 and, in contrast to the large

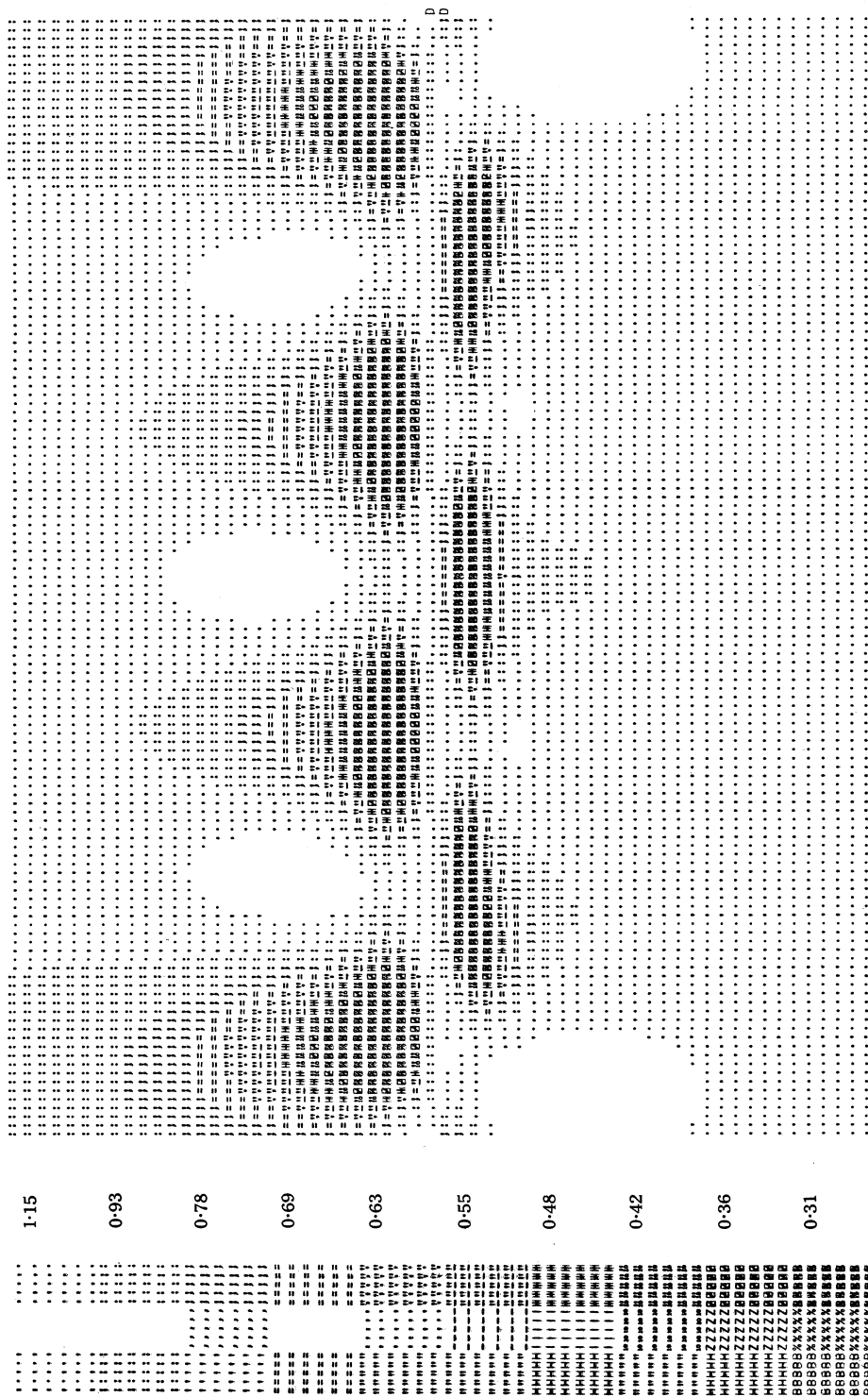
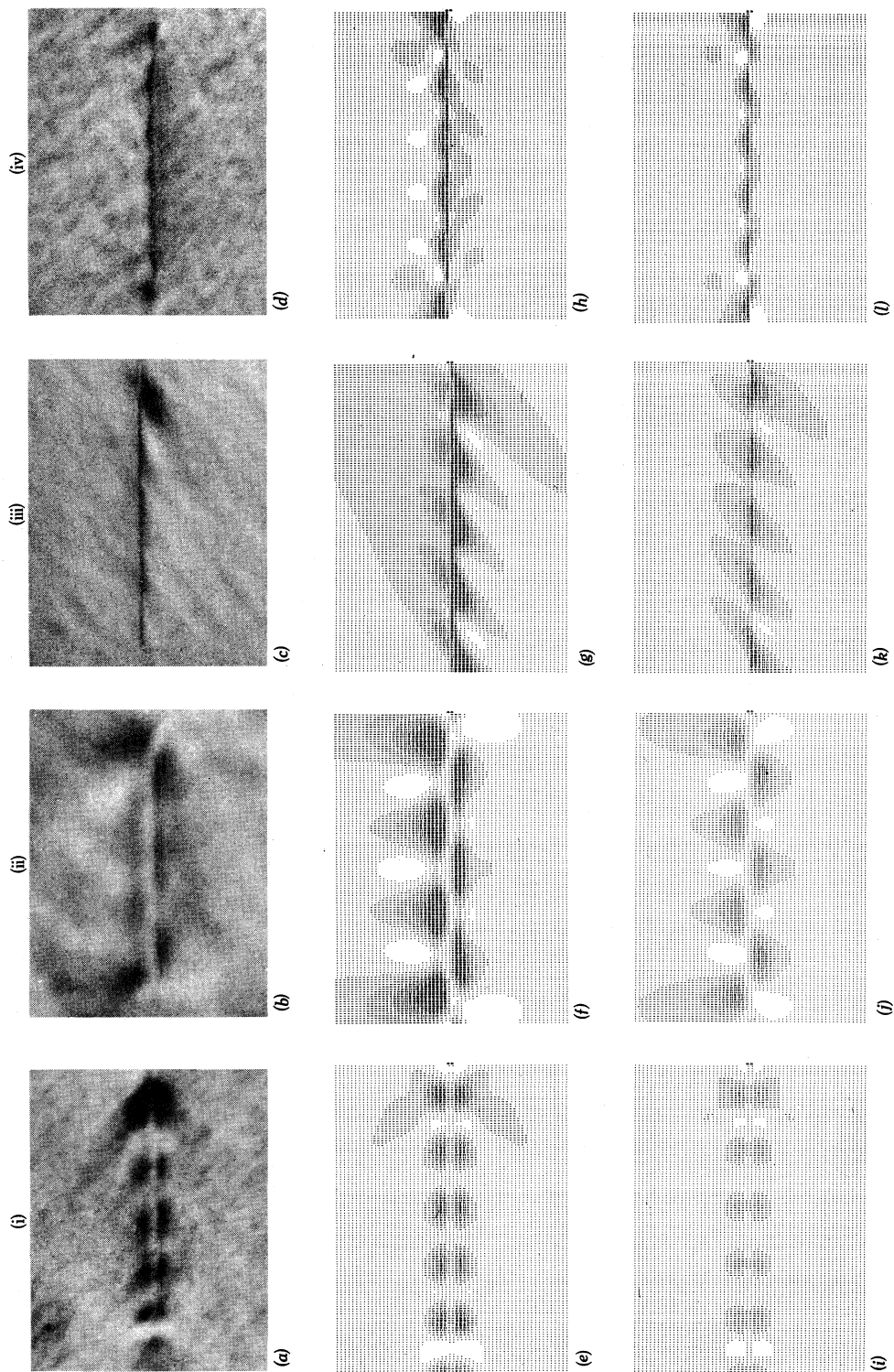
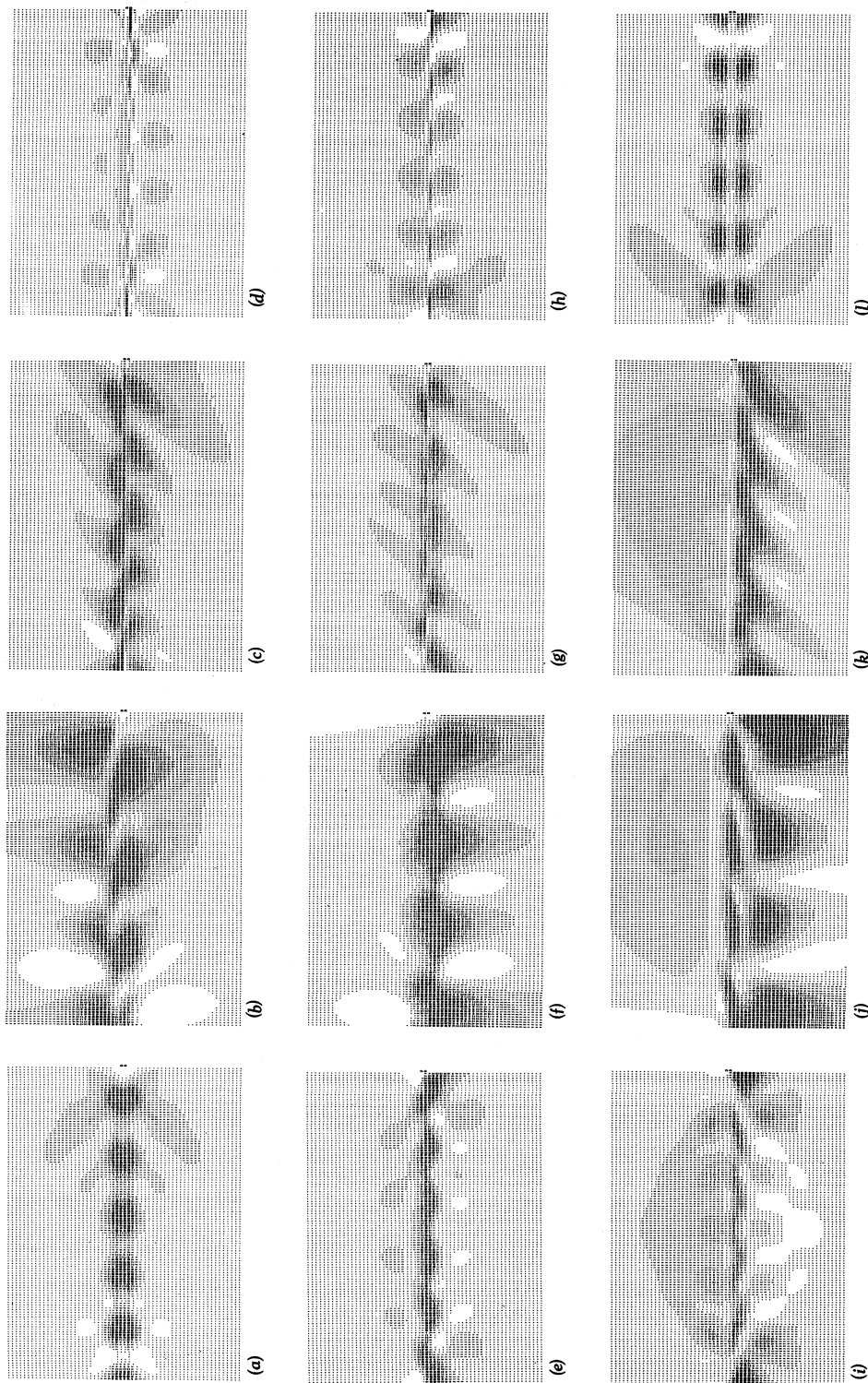


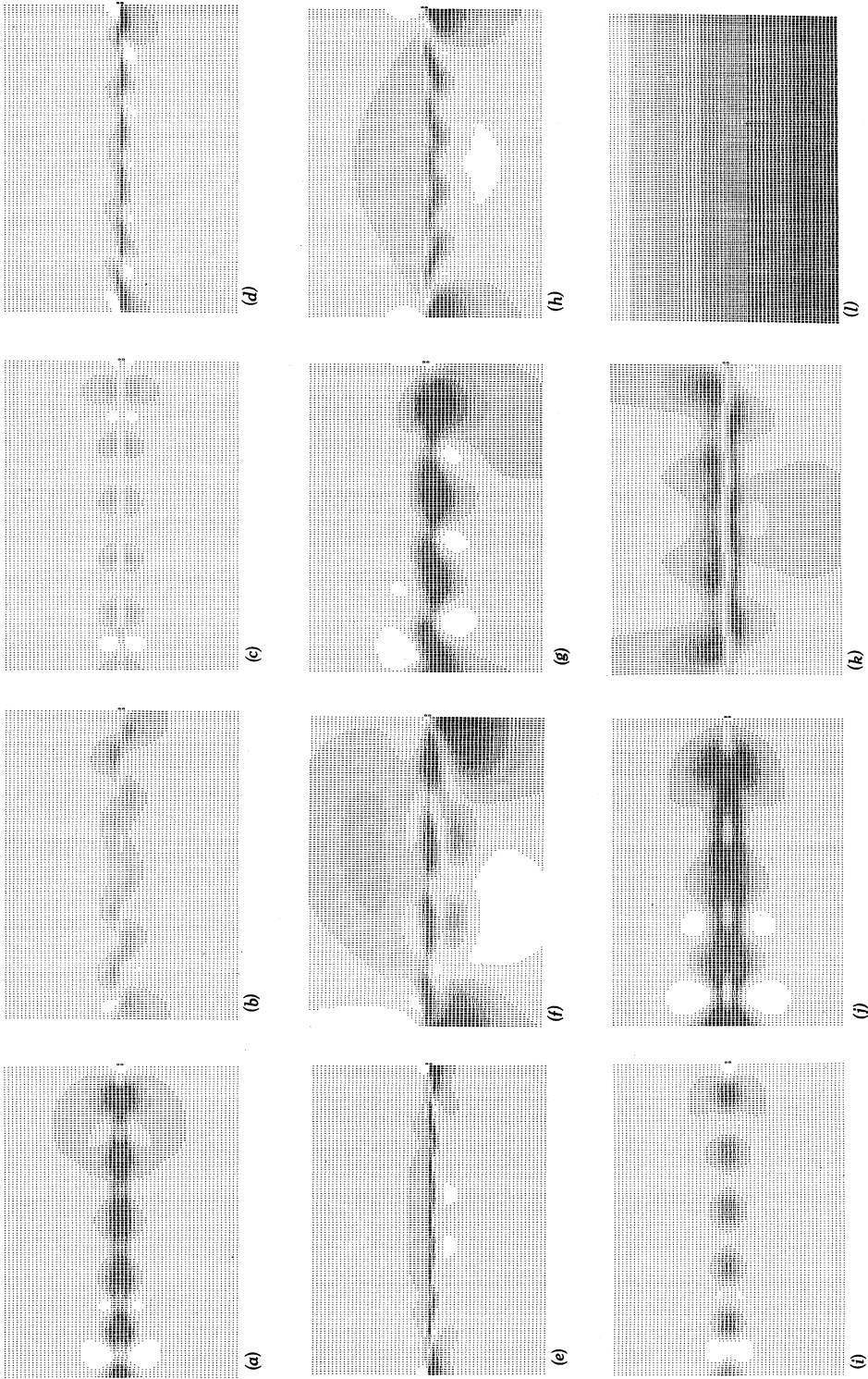
Fig. 1



Figs. 2(a)–2(l)



Figs. 3(a)-3(l)



Figs. 4(a)–4(l)

elastic anisotropy of β -brass, Figure 4 (with one exception) is for isotropic elasticity with a Poisson ratio of 1/3. Four sets of diffracting conditions are considered:

- (i) $[\bar{1}\bar{1}0]_g$, $[001]_{\text{beam}}$, $w = 0.5$, foil thickness = $5\xi_g$;
- (ii) $[\bar{1}\bar{2}1]_g$, $[113]_{\text{beam}}$, $w = 0.7$, foil thickness = $3\xi_g$;
- (iii) $[0\bar{2}0]_g$, $[001]_{\text{beam}}$, $w = 0.7$, foil thickness = $4\xi_g$;
- (iv) $[\bar{1}10]_g$, $[001]_{\text{beam}}$, $w = 0.5$, foil thickness = $5\xi_g$;

and all pictures are bright field images.

Each line of four pictures in Figures 2 and 3 is for a particular Burgers vector viewed under the above four diffracting conditions in the order (i) to (iv). Figures 2(a)–2(d) are experimental pictures of the commonest dislocation in β -brass, which has been shown to be a pure screw dislocation with $\mathbf{b} = [\bar{1}11]$ (Head, Loretto, and Humble 1967a), and Figures 2(e)–2(h) are the corresponding theoretical pictures. In comparing these figures possible differences in the photographic variables of magnification, exposure, and contrast and in the non-uniform background of the experimental pictures must be allowed for. The experimental pictures were printed from the wrong side of the negative to agree with the convention that the pictures are as they appear on the screen of the microscope. Figures 2(i)–2(l) are for the screw dislocation $\mathbf{b} = \frac{1}{2}[\bar{1}11]$, and although there are many similarities with Figures 2(e)–2(h) it is considered that there are sufficient differences to be experimentally distinguishable. Figures 3(a)–3(d) are for $\mathbf{b} = [1\bar{1}1]$. Profiles for this dislocation could not be distinguished from those for $\mathbf{b} = [\bar{1}11]$ with any certainty (Head, Loretto, and Humble 1967a), but when the same information is presented as pictures, differences in topology become apparent. Figures 3(e)–3(h) are for $\mathbf{b} = [100]$, a dislocation that also has been found in β -brass. The images are obviously different from those for the three preceding Burgers vectors, and are in good agreement with experiment (Head, Loretto, and Humble 1967b). Figures 3(i)–3(l) are for $\mathbf{b} = [110]$ as an example of a dislocation that has not yet been found in β -brass but that should be readily recognized with a characteristic set of images.

Humble (1967) has compared profiles of dislocations for isotropic and anisotropic elasticity and has suggested that the effects of anisotropy are most pronounced when $\mathbf{g} \cdot \mathbf{b} = 0$. For the diffraction conditions of Figures 2 and 3, pictures have been computed of all 17 Burgers vectors of type $\frac{1}{2}\langle 111 \rangle$, $\langle 111 \rangle$, $\langle 001 \rangle$, and $\langle 110 \rangle$ both for β -brass and for isotropy and these two sets of 68 pictures show general agreement with Humble's suggestion. In Figures 2 and 3, $\mathbf{g} \cdot \mathbf{b} = 0$ for 7 of the 20 pictures. These are Figures 2(e), 2(f), 2(i), and 2(j), for which the isotropic equivalents are predictably blank (being pure screw dislocations), and Figures 3(a), 3(g), and 3(l), which become Figures 4(a), 4(b), and 4(c) respectively for isotropy. Humble gave one example of an image for which $\mathbf{g} \cdot \mathbf{b} \neq 0$ and which was dependent on the degree of anisotropy. This is Figure 3(h), which becomes Figure 4(d) for isotropy. Figure 3(d), which becomes Figure 4(e), shows a similar change. The largest change was found for Figure 3(j), which becomes Figure 4(f) for isotropy, but most images do not change very much and Figures 4(g) and 4(h), which are the equivalents of Figures 3(f) and 3(i), are typical.

Since isotropy is a degenerate case, dislocations with different Burgers vectors can have identical images. An example is shown in Figure 4(i), which is for diffracting conditions (i) and for a Burgers vector either $\frac{1}{2}[\bar{1}\bar{1}1]$, $[001]$, or $[1\bar{1}0]$. A general rule that is often used to identify Burgers vectors is that if $\mathbf{g} \cdot \mathbf{b} = 0$ the image is invisible or weak. This is of course not necessarily true for anisotropic materials like β -brass, nor, as Figure 4(j) shows, even for isotropy. This picture is for $\mathbf{b} = [101]$ and diffracting conditions (ii) and shows strong contrast and characteristic topology.

Since experimental values of w and foil thickness are usually only known approximately, a survey was made to see if any theoretical images were sensitive to these parameters. With one exception, it was found that the effect of changing these parameters was as might be predicted, namely, that the number of repeated units in a picture changes but the overall topology does not. The one sensitive case is shown in Figure 4(k), which is for identical conditions to Figure 2(f) except that the foil thickness is $3.2\xi_g$ instead of $3.0\xi_g$. These typify the two extremes of image of this dislocation for a range of foil thicknesses and w values. Close examination of the corresponding experimental images (Head, Loretto, and Humble 1967a) also shows a variability between these two extremes.

The final picture (Fig. 4(l)) is the grey scale, 6 lines of each of the 10 symbols, and illustrates that as the size of the picture is reduced the number of detectably different shades is also reduced. However, the topology of the pictures is preserved and for many applications this contains much of the useful information.

V. ACKNOWLEDGMENTS

Thanks are due to Dr. M. H. Loretto for electron micrographs, Dr. P. Humble for photometric measurements, and Mr. E. G. Beckhouse for photography.

VI. REFERENCES

- HEAD, A. K., LORETTO, M. H., and HUMBLE, P. (1967a).—*Phys. Status Solidi* **20**, 505.
 HEAD, A. K., LORETTO, M. H., and HUMBLE, P. (1967b).—*Phys. Status Solidi* **20**, 521.
 HOWIE, A., and WHELAN, M. J. (1961).—*Proc. R. Soc. A* **263**, 217.
 HUMBLE, P. (1967).—*Phys. Status Solidi* **21**, 733.
 LANCE, G. N. (1960).—"Numerical Methods for High Speed Computers." p. 56. (Iliffe: London.)